

The dependence of overlap topological charge density on Wilson mass parameter and the topological charge density correlator

Zhen Cheng and Jian-bo Zhang

Department of Physics, Zhejiang University, Zhejiang 310027, P.R. China

(Dated: October 25, 2021)

Abstract

In this paper, we analyze the dependence of the topological charge density from the overlap operator on the Wilson mass parameter in overlap kernel by the symmetric multi-probing source (SMP) method. We observe that the non-trivial topological objects are removed, as the mass decreased. A comparison of topological charge density calculated by the SMP method using fermionic definition with that of bosonic definition by Wilson flow is shown. Two matching procedures for these two methods are used. We find that there is a best match for these two methods with varied Wilson mass. We also show topological charge density on pre-flowed configurations and find that more Wilson flow time is required to reproduce the topological charge density $q(x)$ for UV-filtered configurations. We attempt to obtain the lower bound for the Wilson flow time τ in the calculation of the topological charge density correlator (TCDC), and extract the pseudoscalar glueball mass from the TCDC based on bosonic definition.

I. INTRODUCTION

Topological charge Q and density $q(x)$ play an important role in the study of the non-trivial topological structure of QCD vacuum. Topological properties have important phenomenological implications, such as θ dependence, spontaneous chiral symmetry breaking, and the confinement may also be related to nontrivial topological properties [1–3]. The topology of QCD gauge fields is a non-perturbative issue, therefore, lattice methods are good choice to investigate it from first principles. Lattice QCD is powerful for studying the topological structure of the vacuum. There are many definitions of the topological charge for a lattice gauge field [4–6]. These definitions can be characterized either as gluonic or fermionic. In fermionic definition, topological charge Q is the number of zero modes of the Dirac operator [7, 8]. On the other hand, topological charge can be given by the field strength tensor (gluonic definition) on the lattice, and this definition approaches fermionic definition in the limit $a \rightarrow 0$ [9–11].

Because of the reflection positivity and the pseudoscalar nature of the relevant local operator in Euclidean field theory, the topological charge density correlator (TCDC) is negative at arbitrary non-zero distance. The negativity of the TCDC has non-trivial consequences related to the nature of topological charge structure in QCD vacuum [12], the pseudoscalar glueball mass can be extracted from the TCDC [13] in pure gauge theory. It is well known that large vacuum fluctuations present in the correlator of gluonic observables, and it has much more difficulties in the extraction of glueball masses compared to hadronic masses. In lattice QCD, due to the TCDC has severe singularities and lattice artifacts, a smoothing procedure for the gauge field is needed. It had shown that undersmearing of gauge fields can not fully eliminate lattice artifacts, while oversmearing may wipe out even the negativity character of the correlator [14]. Thus lower bound of smoothing (Wilson flow) is badly needed.

The four-volume integral of the TCDC gives the topological susceptibility χ [15]. The topological susceptibility which reflects the fluctuations of the topological charge is also of great importance in the study of the QCD vacuum. Universality of the topological susceptibility in fermionic definition shows that the topological susceptibility is free of short-distance singularities [16]. The topological susceptibility χ is related to the $U(1)$ anomaly and the mass of the flavour-singlet pseudoscalar η' meson in pure Yang-Mills theory, manifested in

the famous Witten-Veneziano relation [17, 18]. The topological susceptibility can also be used to figure out a lower bound for the flow time [19].

The overlap Dirac operator is a solution of the Ginsparg-Wilson equation [20, 21], and the topological charge defined from the overlap fermion will be an exact integer. In traditional method the point source is used in the calculation of topological charge density [22, 23], so the computation on the large lattice is almost impossible. In order to reduce the computational cost, the symmetric source (SMP) method is introduced to calculate the topological charge density [24]. As the Wilson mass parameter m varies, the value of Q may change [25–28]. The topological charge density $q(x)$ has strong correlation with low-lying modes of the Dirac operator, which strongly influence how quark propagate through the vacuum. So the topological charge density $q(x)$ is a useful probe of the gauge field. We visualize the topological charge density and view the detailed extra information [29]. On the other hand, the topological charge can not show the details of the QCD vacuum, and the topological charge density $q(x)$ in the study of the topological properties of the QCD vacuum will be analyzed. We will show an analysis of the topological charge $q(x)$, as Wilson mass parameter m and Wilson flow time τ vary. We consider all time slices and show more details on the topological charge density with different topological charge, which is different from the single time-slice studied in the Ref. [30]. By analyzing the topological charge density $q(x)$, we can obtain a great amount of information about the underlying topological structure. We show a comparison with the gluonic topological charge density that is calculated after the application of Wilson flow algorithm. Two matching methods are considered in this paper. The first method is to compare the two definitions of the topological charge density by applying a multiplicative renormalization to the gluonic topological charge density. The second one is to calculate a parameter Ξ_{AB} , and the best match will be reached when Ξ_{AB} is nearest to 1.

We will also analyze the properties of topological charge density by using the SMP method on the pre-smoothed configuration.

Finally, we will try to show the best radius of the Wilson flow by analyzing the matching procedure between two definitions of topological charge density and the stability of the topological susceptibility, and then we try to extract the psuedoscalar glueball mass from the TCDC of pure gauge theory.

II. SIMULATION DETAILS

The pure gauge lattice configurations, generated using a tadpole improved, plaquette plus rectangle gauge action through pseudo-heat-bath algorithm [31, 32]. This gauge action at tree-level $\mathcal{O}(a^2)$ -improved is defined as

$$S_G = \frac{5\beta}{3} \sum_{\substack{x\mu\nu \\ \nu > \mu}} \text{Re Tr} [1 - P_{\mu\nu}(x)] - \frac{\beta}{12u_0^2} \sum_{\substack{x\mu\nu \\ \nu > \mu}} \text{Re Tr} [1 - R_{\mu\nu}(x)] \quad (1)$$

where $P_{\mu\nu}$ is the plaquette term. The link product $R_{\mu\nu}(x)$ denotes the rectangular 1×2 and 2×1 plaquettes. The mean link, u_0 is the tadpole improvement factor that largely corrects for the quantum renormalization of coefficient for the rectangles relative to the plaquette and is given by

$$u_0 = \left(\frac{1}{3} \text{Re Tr} \langle P_{\mu\nu}(x) \rangle \right)^{1/4}. \quad (2)$$

In the fermionic definitions, we use the overlap operator to calculate topological charge density. The massless overlap Dirac operator is given by [28]

$$D_{\text{ov}} = \left(\mathbb{1} + \frac{\gamma_5 D_W}{\sqrt{D_W^\dagger D_W}} \right), \quad (3)$$

where D_W is the Wilson Dirac operator,

$$D_W = \delta_{a,b} \delta_{\alpha,\beta} \delta_{m,n} - \kappa \sum_{\mu=1}^4 [(\mathbb{1} - \gamma_\mu)_{\alpha\beta} \times U_\mu(m)_{ab} \delta_{m,n-\hat{\mu}} + (\mathbb{1} + \gamma_\mu)_{\alpha\beta} \times U_\mu^\dagger(m - \hat{\mu})_{ab} \delta_{m,n+\hat{\mu}}], \quad (4)$$

which is the kernel of the overlap operator and κ is the hopping parameter,

$$\kappa = \frac{1}{2(-m + 4)}, \quad (5)$$

and in the overlap formalism κ has to be in the range $(\kappa_c, 0.25)$ for D_{ov} to describe a single massless Dirac fermion, where κ_c is the critical value of κ at which the pion mass extrapolates to zero in the simulation with ordinary Wilson fermions. We call m as the Wilson mass parameter. In this work, we choose parameter κ as the input parameter.

The overlap topological charge density can be calculated as follows,

$$q_{\text{ov}}(x) = \frac{1}{2} \text{Tr}_{c,d}(\gamma_5 D_{\text{ov}}(x)) = \text{Tr}_{c,d}(\tilde{D}_{\text{ov}}(x)), \quad (6)$$

where the trace is over the color and Dirac indices. It is well known that the point source is used to get $q_{\text{ov}}(x)$ in the traditional method, but calculation of $q_{\text{ov}}(x)$ with point source is almost impossible for the large lattice volume.

In order to avoid the high computational effort in the calculation of the $q(x)$ with point source, we apply the symmetric multi-probing (SMP) method to calculate $q(x)$ [24],

$$\begin{aligned} q_{\text{smp}}(x) &= \sum_{\alpha,a} \psi(x, \alpha, a) \left(\tilde{D}_{\text{ov}}(x) \right) \phi_P(S(x, P), \alpha, a) \\ &= \sum_{\alpha,a} \psi(x, \alpha, a) \left(\tilde{D}_{\text{ov}}(x) \right) \psi(x, \alpha, a) \\ &\quad + \sum_{y \in S(x, P)} \sum_{\alpha,a}^{y \neq x} \psi(x, \alpha, a) \left(\tilde{D}_{\text{ov}}(x) \right) \psi(y, \alpha, a), \end{aligned} \quad (7)$$

where $S(x, P)$ represents the sites with the same color of x obtained by the symmetric coloring scheme $P\left(\frac{n_s}{d}, \frac{n_s}{d}, \frac{n_s}{d}, \frac{n_t}{d}, \text{mode}\right)$. n_s and n_t are the spatial and temporal sizes of the lattice, d is the minimal distance and $\text{mode} = 0, 1, 2$ corresponds to the Normal, Split and Combined mode for scheme P [33]. x is the seed site at site (x_1, x_2, x_3, x_4) and y are the other lattice sites belong to the set $S(x, P)$. $\phi_P(S(X, P), \alpha, a)$ is the SMP source vector, and ψ is the normalized point source vector. The second term in eq. (7) is the sum of off-diagonal components of \tilde{D}_{ov} which has the space-time locality [23, 34], so this term can be regard as the error in the evaluation of topological charge density. If we choose the proper scheme P of the SMP source, the error will be quite small. In this case, we can neglect the error term and get

$$\begin{aligned} q_{\text{smp}}(x) &= \sum_{\alpha,a} \psi(x, \alpha, a) \left(\tilde{D}_{\text{ov}}(x) \right) \phi_P(S(x, P), \alpha, a) \\ &= \sum_{\alpha,a} \psi(x, \alpha, a) \left(\tilde{D}_{\text{ov}}(x) \right) \psi(x, \alpha, a). \end{aligned} \quad (8)$$

We will analyse $q(x)$ on lattice $24^3 \times 48$ at the inverse coupling, $\beta = 4.8$. We show the visualization of the topological charge density of two configurations and apply two matching procedures to obtain the best flow time τ in the calculation of topological charge density. We will also analyze the topological properties of the pre-flowed configurations.

In addition, we will analyze the TCDC and try to extract the pseudoscalar glueball mass from the TCDC. Because of too much computational cost to calculate $q(x)$ by using the SMP method with large distance d for lots of configurations, we choose the gluonic definition to calculate the TCDC with Wilson flow algorithm. TCDC is calculated on $24^3 \times 48$ lattice with $\beta = 4.8$, corresponding to the lattice space $a = 0.0845$ fm. In the evaluation of TCDC, the number of configurations is $N_{\text{conf}} = 500$.

III. $q(x)$ FOR DIFFERENT METHODS

Before we proceed the analysis, we first demonstrate that the SMP method with proper d is a good method to evaluate the topological density with overlap Dirac operator. Due to the high computational cost, we only make a comparison of the point source and the SMP source in eq. (6) on $12^3 \times 24$ lattice with $\beta = 4.8$, $\kappa = 0.21$. We shown $q_{\text{ps}}(x)$ by the point source method and $q_{\text{smp}}(x)$ by the SMP method with $d = 6$ in Fig. 1. It shows that $q_{\text{smp}}(x)$ is highly matched with $q_{\text{ps}}(x)$. The matching parameter Ξ_{AB} , defined in the following page, for these two methods is 0.9997, and we can barely see the difference by naked eyes. Thus the SMP method is good choice to calculate the topological charge density while the parameter d is large enough. It is expected that the larger distance d , the better match [24].

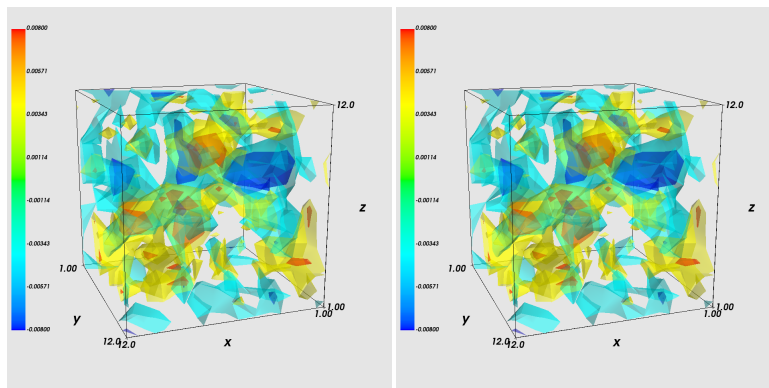


Figure 1: $q_{\text{ps}}(x)$ and $q_{\text{smp}}(x)$ on lattice $L = 12^3 \times 24$ by the point source and SMP source for the $t = 12$ slice, other time slices are similar. To the naked eyes, they are almost the same. The parameters, $\kappa = 0.21$ and $\beta = 4.80$, are the same for both. Left: Point source, Right: SMP source.

In order to obtain more precise topological charge density, we choose the distance param-

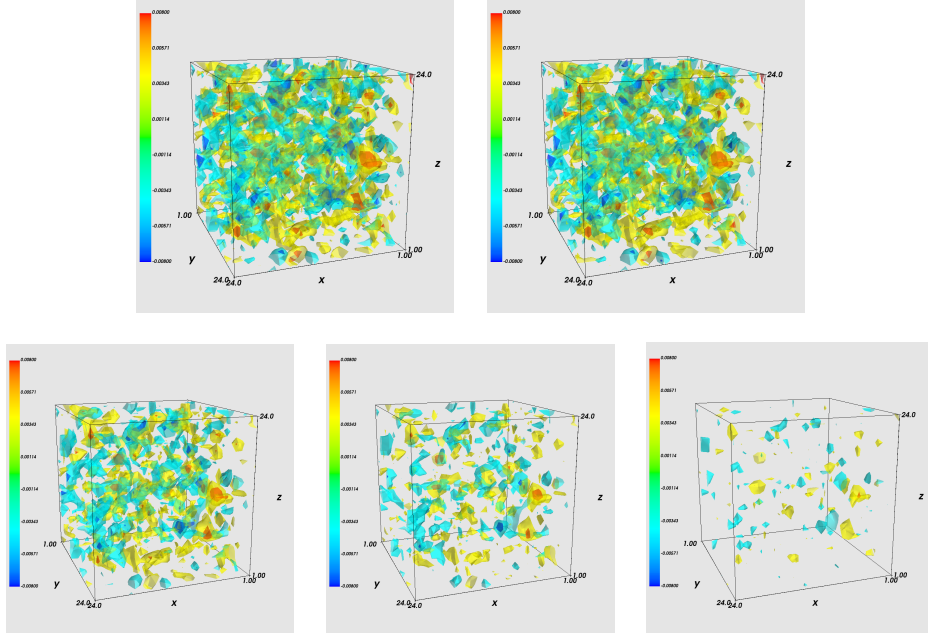


Figure 2: The SMP topological charge density $q_{\text{smp}}(x)$ of time slice $t = 24$ calculated by the SMP method with five choices for the Wilson hopping parameter κ of conf. 1. From left to right, the parameter $\kappa = 0.23$ and 0.21 on the first row, with 0.19 , 0.18 and 0.17 on the second. $q_{\text{smp}}(x)$ depends on the parameter κ , and larger κ reveals more topological charge density.

eter $d = 8$ in the SMP method on $24^3 \times 48$ lattice. In these calculations of $q(x)$ by the SMP method, we find that the topological charge Q is not always the same for different κ values, as is shown in Table. I and II. This is acceptable, zero crossings in the spectral flow of the $\tilde{D}_{\text{ov}}(x)$ occur for different κ on lattice [6, 26]. It indicates that even though topological charge Q from overlap fermion is always an integer, but its value is not unique, and it has a dependence on Wilson mass parameter m in the overlap kernel. The $q_{\text{smp}}(x)$ with $d = 8$ of five different $\kappa = 0.17, 0.18, 0.19, 0.21$ and 0.23 for two configurations (conf. 1 and 2) are shown in the Fig. 2 and 3. It indicates that $q_{\text{smp}}(x)$ has very clear dependence on the parameter κ . The larger κ reveals much more topological charge density. All these figures show that as the κ is decreased, the non-trivial topological objects are removed, which has a resemblance to the smoothing algorithms. We can also see that the maximal (minimal) values of $q_{\text{smp}}(x)$ emerge almost at the same position.

Gradient flow is a non-perturbative smoothing procedure, which has been proven to have well-defined numerically and perturbatively properties. If the fields are smoothed via gradient flow, they do not need to be renormalized. The key idea of gradient flow is a

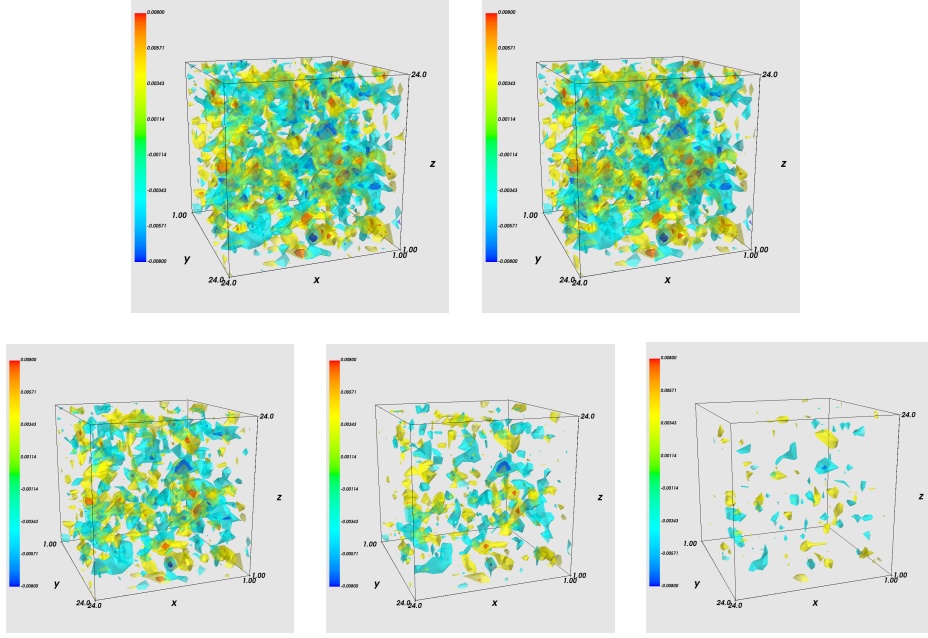


Figure 3: The SMP topological charge density $q_{\text{smp}}(x)$ of time slice $t = 24$ calculated by the SMP method with five choices for the Wilson hopping parameter κ of conf. 2. From left to right, the parameter $\kappa = 0.23$ and 0.21 on the first row, with 0.19 , 0.18 and 0.17 on the second. $q_{\text{smp}}(x)$ has a dependence on the parameter κ , and smaller κ show less topological charge density.

smoothing of the original gauge field towards stationary points of the action.

The gradient flow is defined as the solution of the evolution equations [6, 35, 36]

$$\dot{V}_\mu(x, \tau) = -g_0^2 [\partial_{x,\mu} S_G(V(\tau))] V_\mu(x, \tau), \quad V_\mu(x, 0) = U_\mu(x), \quad (9)$$

where τ is the dimensionless gradient flow time and the link derivative is defined by

$$\begin{aligned} \partial_{x,\mu} S_G(U) &= i \sum_a T^a \frac{d}{ds} S_G(e^{isY^a} U) \Big|_{s=0}, \\ &\equiv i \sum_a T^a \partial_{x,\mu}^{(a)} S_G(U). \end{aligned} \quad (10)$$

In this expression, T^a is the Hermitian generators of the $\text{SU}(N)$ ($\text{SU}(3)$ in our work) algebra, with the normalization $\text{Tr}(T^a T^b) = \frac{1}{2} \delta^{ab}$, and

$$Y^a(y, \nu) = \begin{cases} T^a & \text{if } (y, \nu) = (x, \mu), \\ 0 & \text{else.} \end{cases} \quad (11)$$

If we introduce the notation $\Omega_\mu = U_\mu(x) X_\mu^\dagger(x)$, we obtain

$$\partial_{x,\mu}^{(a)} S(U) = \frac{1}{g_0^2} \text{Im Tr} [T^a \Omega_\mu], \quad (12)$$

where $X_\mu^\dagger(x)$ is the so-called staples, defined by

$$\begin{aligned} X_\mu^\dagger(x) = & \sum_{\nu \geq 0, \nu \neq \mu} [U_\mu(x) U_\mu(x + \hat{\nu}) U_\nu^\dagger(x + \hat{\mu}) \\ & + U_\nu^\dagger(x - \hat{\nu}) U_\mu(x - \hat{\nu}) U_\mu(x - \hat{\nu} + \hat{\mu})], \end{aligned} \quad (13)$$

and $g_0^2 \partial_{x,\mu} S(U)$ is given by

$$\begin{aligned} g_0^2 \partial_{x,\mu} S(U) = & 2i \sum_a T^a \text{Im Tr} [T^a \Omega_\mu] \\ = & \frac{1}{2} (\Omega_\mu(x) - \Omega_\mu^\dagger) - \frac{1}{2N} \text{Tr} (\Omega_\mu(x) - \Omega_\mu^\dagger). \end{aligned} \quad (14)$$

In practice, the gradient flow moves the gauge configuration along the steepest descent direction in the configuration space, such as along the gradient of the action. The chosen sign in the evolution equations leads to a minimization of the action, which is as expected. We use the third order Runge-Kutta method to obtain the solution of the flow Eq. (9). After Wilson flow, the gluonic definition of topological charge density, $q_{\text{wf}}(x)$ is given by

$$q_{\text{wf}}(x) = \frac{1}{32\pi^2} \epsilon_{\mu\nu\rho\sigma} \text{Tr} [F_{\mu\nu} F_{\rho\sigma}], \quad (15)$$

where the field-strength tensor $F_{\mu\nu}$ used in this work is a 3-loop $\mathcal{O}(a^4)$ -improved and defined by [37],

$$F_{\mu\nu}^{\text{Imp}} = \frac{27}{18} C^{(1,1)} - \frac{27}{180} C^{(2,2)} + \frac{1}{90} C^{(3,3)}, \quad (16)$$

and $C^{(m,n)}$ denotes the three $m \times n$ loops used to construct the clover term.

In order to fairly compare the two definitions for the topological charge density with the varied Wilson mass parameter. Two matching procedures are introduced[30]. The first matching method is to find the factor Z_{fit} , which is satisfied

$$\min \sum (q_{\text{smp}}(x) - Z_{\text{fit}} q_{\text{wf}}(x))^2. \quad (17)$$

We also calculate the factor Z_{calc} , defined as

$$Z_{\text{calc}} \equiv \frac{\sum_x |q_{\text{ov}}(x)|}{\sum_x |q_{\text{wf}}(x)|}. \quad (18)$$

The second matching procedure is to calculate the quantity Ξ_{AB} , given by [38]

$$\Xi_{AB} = \frac{\chi_{AB}^2}{\chi_{AA}\chi_{BB}}, \quad (19)$$

with

$$\chi_{AB} = \frac{1}{V} \sum_x (q_A(x) - \bar{q}_A)(q_B(x) - \bar{q}_B), \quad (20)$$

where \bar{q} denotes the mean value of $q(x)$, and in this work $q_A(x) \equiv q_{\text{smp}}(x)$, $q_B(x) \equiv q_{\text{wf}}(x)$. When the Ξ_{AB} is nearest 1, the best match is found.

The $q_{\text{wf}}(x)$ at $n_t = 24$ with integration step $\epsilon = 0.005$ for flow time $\tau = 0, 0.1, 0.2, 0.3$ and 0.4 are shown in Fig. 4 and 5. We see that the non-trivial topological charge fluctuations are removed as the flow time is increased, which has the same tendency as cooling and stout-link smearing algorithm [28, 32, 37, 39, 40].

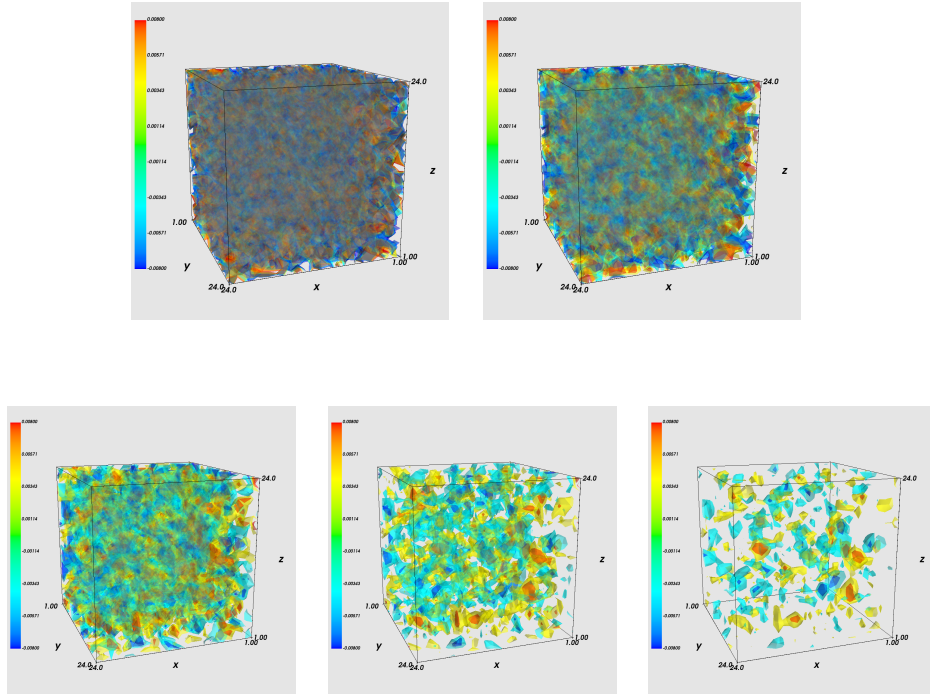


Figure 4: The gluonic topological charge density $q_{\text{wf}}(x)$ of time slice $t = 24$ calculated after Wilson flow for conf. 1. Flow time $\tau = 0, 0.1$ on the first row from left to right, with $\tau = 0.2, 0.3$ and 0.4 on the second.

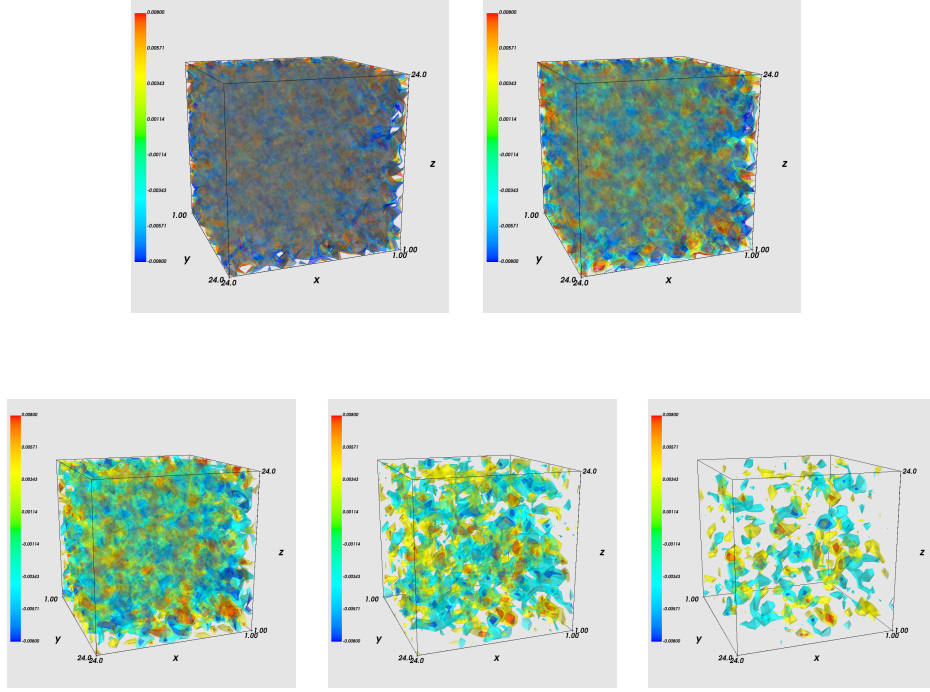
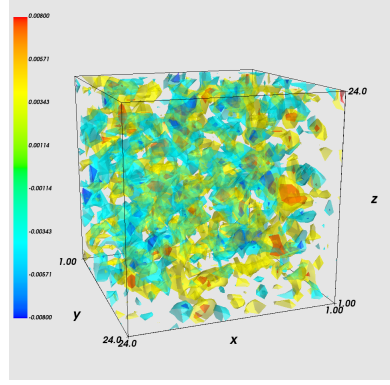
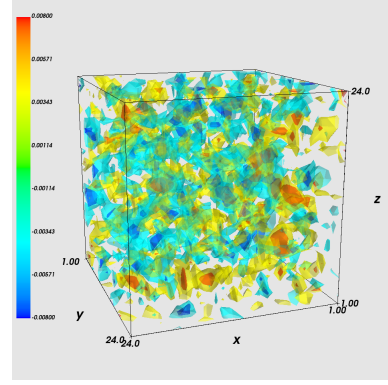


Figure 5: The gluonic topological charge density $q_{\text{wf}}(x)$ of time slice $t = 24$ calculated after Wilson flow for conf. 2. Flow time $\tau = 0, 0.1$ on the first row from left to right, with $\tau = 0.2, 0.3$ and 0.4 on the second.

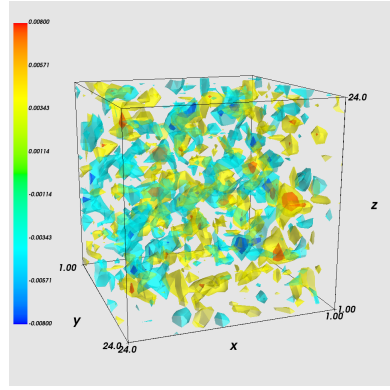
The SMP topological charge density for three choices κ compared with the best matching number of Wilson flow, n_{wf} , are shown in Fig. 6 and 7, and $q_{\text{wf}}(x)$ is renormalized using Z_{calc} . It finds that the best matching number of Wilson flow for the two matching methods is the same for the same configuration. It shows that more Wilson flow time for $q_{\text{wf}}(x)$ are needed to match the topological charge density $q_{\text{smp}}(x)$ when κ is decreased. It indicates that the $q_{\text{smp}}(x)$ is less sensitive to small objects as κ is decreased, and the non-trivial topological charge can be removed by Wilson flow smoothing.



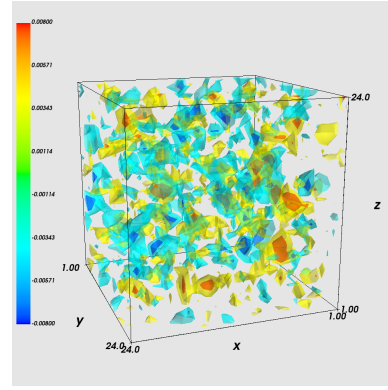
$$\kappa = 0.23$$



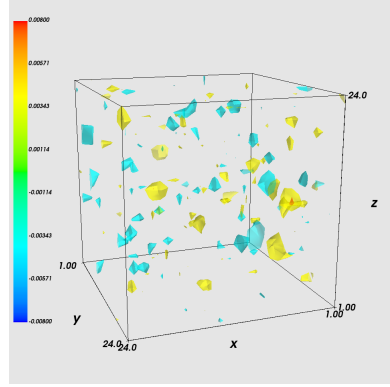
$$n_{\text{wf}} = 59$$



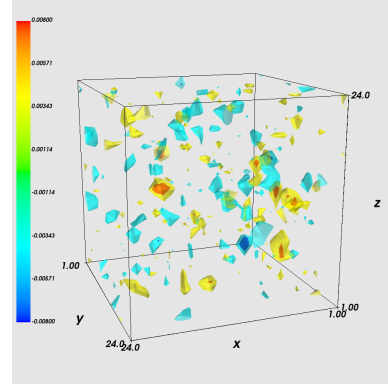
$$\kappa = 0.19$$



$$n_{\text{wf}} = 65$$



$$\kappa = 0.17$$



$$n_{\text{wf}} = 73$$

Figure 6: The best flowed topological charge density $q_{\text{wf}}(x)$ compared with the overlap $q_{\text{smp}}(x)$ for the time slice $t = 24$ of conf. 1, where $q_{\text{wf}}(x)$ is renormalized using Z_{calc} . Smaller κ values require larger number of Wilson flow to reproduce the topological charge density. n_{wf} is the best matching number of Wilson flow.

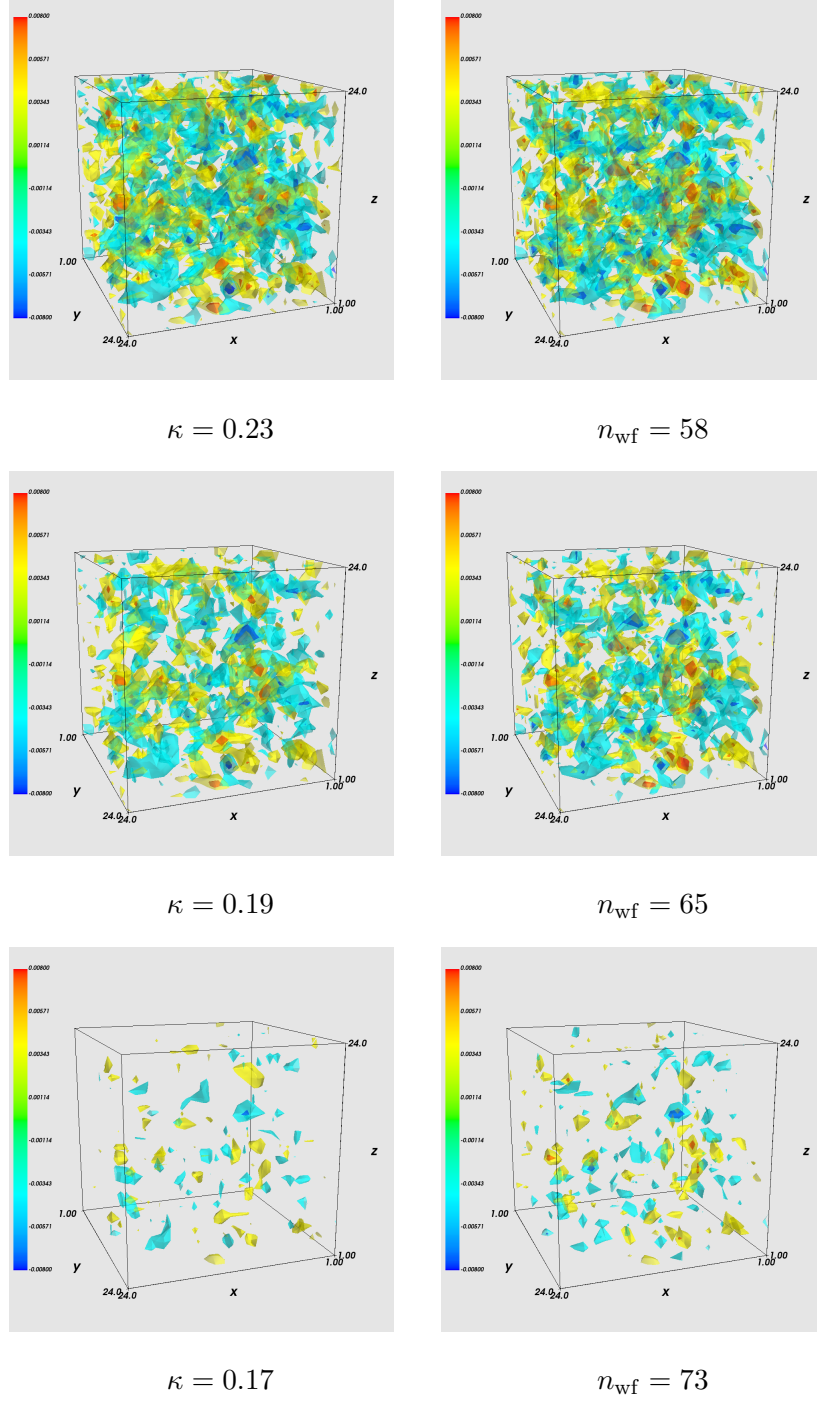


Figure 7: The best flowed topological charge density $q_{\text{wf}}(x)$ renormalized by using Z_{calc} , compared with the SMP topological charge density $q_{\text{smp}}(x)$ for the time slice $t = 24$ of conf. 2. Larger κ values require smaller number of Wilson flow to reproduce the topological charge density. n_{wf} represents the best matching number of Wilson flow.

Ξ_{AB} , Z_{calc} and Z_{fit} of two configurations for five different κ are shown in Table I and II,

κ	n_{wf}	Z_{calc}	Z_{fit}	Ξ_{AB}	Q_{smp}
0.17	73	0.6811	0.5671	0.7653	8.0077
0.18	69	0.8364	0.7018	0.7670	7.0078
0.19	65	0.9275	0.7781	0.7580	7.0095
0.21	61	1.0215	0.8490	0.7324	9.0169
0.23	59	0.9811	0.7999	0.6972	9.0279

Table I: The best matching number of Wilson flow, n_{wf} , needed to match the SMP topological charge density with different κ for conf. 1. n_{wf} is the same for the two matching procedure. Q obtained by SMP method are different for varied κ .

κ	n_{wf}	Z_{calc}	Z_{fit}	Ξ_{AB}	Q_{smp}
0.17	73	0.6802	0.5668	0.7661	4.9938
0.18	69	0.8359	0.7005	0.7656	4.9932
0.19	65	0.9274	0.7776	0.7574	3.9942
0.21	61	1.0211	0.8467	0.7309	3.9949
0.23	58	0.9596	0.7810	0.6953	3.9967

Table II: The best matching number of Wilson flow, n_{wf} , needed to match the SMP topological charge density with varied κ for conf. 2. n_{wf} is the same for the two matching procedure. Q obtained by SMP method are different for varied κ .

respectively. It finds that the two matching procedures is consistent and the best matching number of Wilson flow is the same for the same κ . It shows that Ξ_{AB} , Z_{calc} and Z_{fit} are independent of topological charge Q , and almost equal for different configurations with the same κ . We note that the two matching procedures has almost the same n_{wf} for these two configurations. It also shows that the best match of the first matching procedure is nearly independent of topological charge Q . The best match of first matching method for different configurations, has almost the same n_{wf} when κ is equal.

In Fig. 8, Ξ_{AB} versus the number of Wilson flow is shown. We see that as the number of Wilson flow n_{wf} increases, Ξ_{AB} reaches to a maximum value and then decreases. We can also observe that the best match has the same n_{wf} for the same κ and is independent of the

configurations. We can see that for different κ , the best matching number of Wilson flow n_{wf} is different. However, it is reasonable to choose the average value of the best matching number of Wilson flow of different κ as the best n_{wf} , and it is about $n_{\text{wf}} = 65$ or Wilson flow radius $\sqrt{8\tau} \approx 0.136 \text{ fm}$ for gluonic $q_{\text{wf}}(x)$ to match with fermionic $q_{\text{smp}}(x)$.

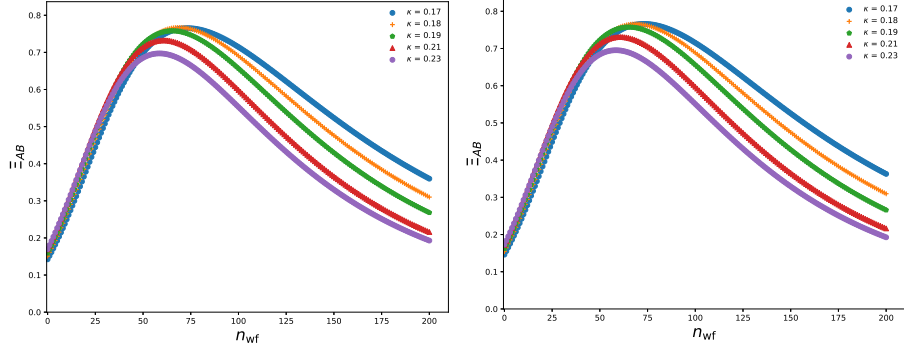


Figure 8: Ξ_{AB} versus the number of Wilson flow n_{wf} for different κ of two configurations. As κ is decreased, the best matching number of Wilson flow is increased. Left: conf. 1. Right: conf. 2

IV. $q(x)$ ON UV-FILTERED CONFIGURATIONS

In this section, we will discuss the effect of calculating the SMP topological charge density $q_{\text{smp}}(x)$ on the UV-filtered configurations, that is, before calculating the topological charge density, we smooth the configuration by using Wilson flow. We used $q_{\text{smp}}^{\text{UV}}(x)$ to denote the topological charge density calculated by using the SMP method on pre-smoothed configurations. We are interested in whether much more smoothing procedures will be needed for the pre-smoothed configurations to match with $q_{\text{smp}}(x)$ or whether the topological charge value will be more stable for different κ .

κ	n_{wf}	Z_{calc}	Z_{fit}	Ξ_{AB}	Q_{smp}
0.17	130	0.8980	0.8374	0.9386	7.0030
0.18	122	0.9080	0.8525	0.9364	7.0036
0.19	115	0.8922	0.8450	0.9346	8.0041
0.21	110	0.8124	0.7758	0.9253	8.0047
0.23	110	0.6146	0.5939	0.8975	8.0035

Table III: The best matching number of Wilson flow, n_{wf} , needed to match the SMP topological charge density with different κ for the pre-flowed conf.1. n_{wf} for the two matching procedures is same. Q with varied κ is not the same.

κ	n_{wf}	Z_{calc}	Z_{fit}	Ξ_{AB}	Q_{smp}
0.17	129	0.8873	0.8275	0.9418	4.9971
0.18	121	0.8963	0.8412	0.9399	4.9959
0.19	114	0.8792	0.8289	0.9360	4.9942
0.21	109	0.7994	0.7588	0.9281	4.9891
0.23	106	0.5894	0.5640	0.9054	4.9847

Table IV: The best matching number of Wilson flow, n_{wf} , needed to match the SMP topological charge density with different κ for the second pre-flowed conf.2. n_{wf} for the two matching procedures is same. Q of varied κ is the same.

In Table. III and IV, Ξ_{AB} , Z_{calc} and Z_{fit} for two pre-flowed configurations with different κ are shown. It shows that the best matching number of Wilson flow, n_{wf} , for the two matching procedures is the same, which has the same properties with the original configurations. The pre-flowed number of Wilson flow of two configurations for different κ is provided by the matching procedures in the previous analysis. It shows that the topological charge Q of pre-flowed configurations may be different from Q of the original configurations. Q of the pre-flowed configurations tend to be more stable than that of original configurations as κ varied, which is as respected. It can be attributed to that the Wilson flow can remove the non-trivial topological charge density fluctuations. It also indicates that more Wilson flow

time will be required to match $q_{\text{smp}}^{\text{UV}}(x)$.

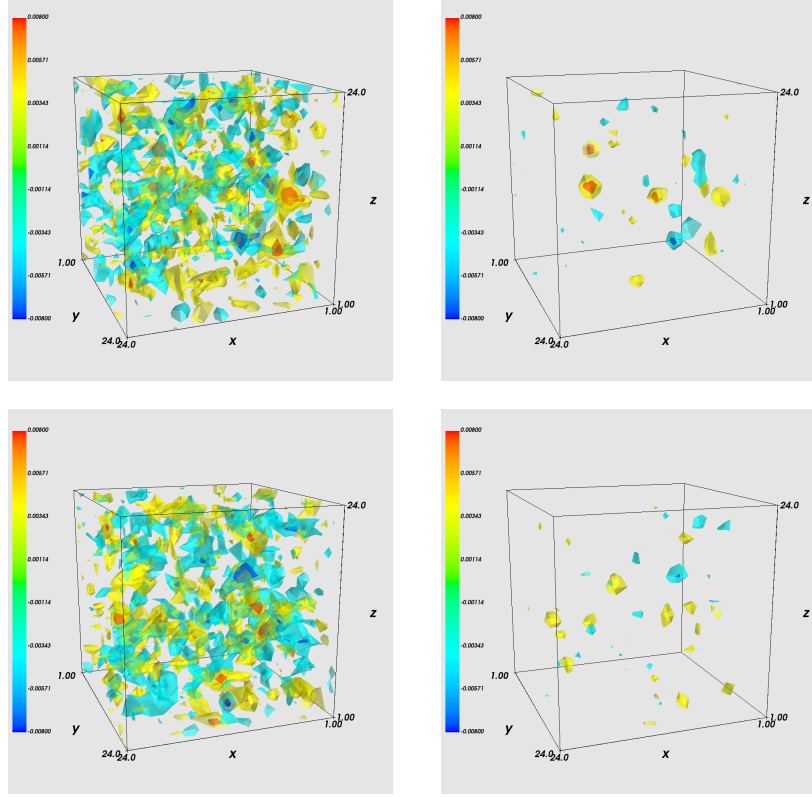


Figure 9: A comparison of $q_{\text{smp}}(x)$ with $q_{\text{smp}}^{\text{UV}}(x)$ using the same κ for time slice $t = 24$ of two configurations. Left: $q_{\text{smp}}(x)$ evaluated with $\kappa = 0.19$. Right: $q_{\text{smp}}^{\text{UV}}(x)$ calculated with the same κ , after Wilson flow with $n_{\text{wf}} = 65$. Far less topological charge density are observed in the pre-flowed configurations. Top: conf. 1. Bottom: conf. 2.

In Fig. 9, we show a comparison of $q_{\text{smp}}(x)$ with $q_{\text{smp}}^{\text{UV}}(x)$ for $\kappa = 0.19$ and the best matching number of Wilson flow is $n_{\text{wf}} = 65$ for the pre-smoothed configurations. Much less topological charge density is observed in the pre-smoothed case, and the pre-flowed operation has the similar effect to the Wilson flow. It is clear that a much larger number of Wilson flow will be required to reproduce $q(x)$ using the gluonic definitions.

By doing the same matching process as before, we find that $n_{\text{wf}} = 115$ and 114 of Wilson flow provides the best match to the SMP topological charge density on these two pre-smoothed configurations respectively. A comparison of $q_{\text{smp}}^{\text{UV}}(x)$ with $q_{\text{wf}}(x)$ is shown in Fig. 10. It shows that much more Wilson flow time is required to match the SMP topological charge density, as expected. These results show that the filtering function that the SMP

method played is independent of the input gauge field.

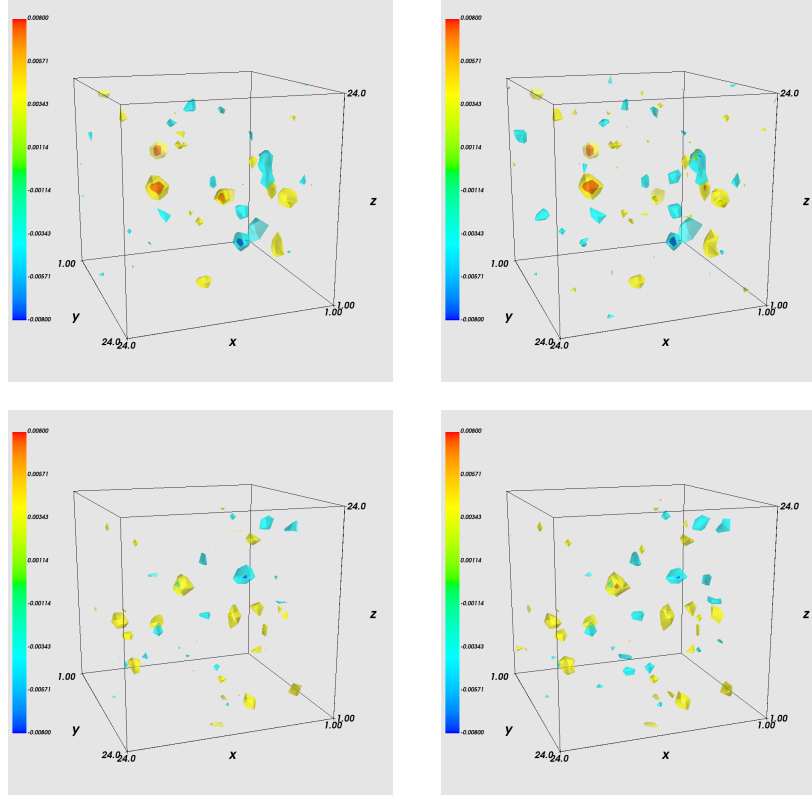


Figure 10: $q_{\text{smp}}^{\text{UV}}(x)$ evaluated on two configurations smoothed by Wilson flow with $n_{\text{wf}} = 65$, compared with Wilson flow topological charge density $q_{\text{wf}}(x)$ renormalized by using Z_{calc} and time slice is $t = 24$. The best matching number of Wilson flow is $n_{\text{wf}} = 115$ and 114 for conf.1 and 2 respectively. $q_{\text{smp}}^{\text{UV}}(x)$ looks almost the same with $q_{\text{wf}}(x)$ renormalized by using Z_{calc} for the best match. Top: conf.1. Bottom: conf.2.

Ξ_{AB} of the pre-flowed configurations is shown in Fig. 11. Ξ_{AB} for pre-flowed configurations has the similar pattern to the configurations without pre-flowed. However, the best match of pre-flowed configurations for different κ has much larger n_{wf} , and the maximum number of Wilson flow is even $n_{\text{wf}} = 130$. It also indicates that the best matching is improved by the pre-flowed process.

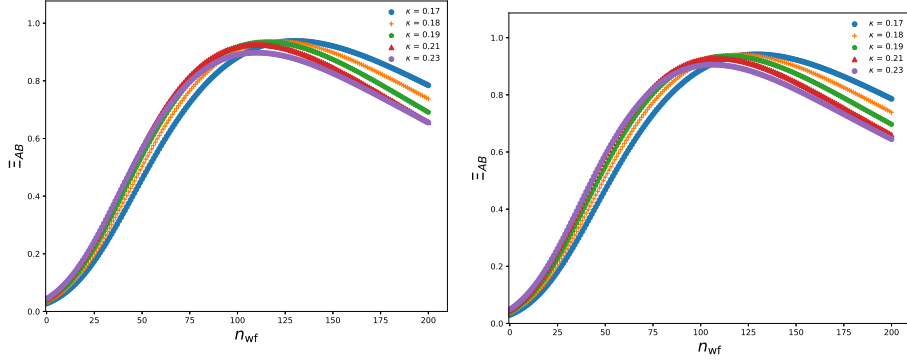


Figure 11: Ξ_{AB} versus the number of Wilson flow n_{wf} for different κ . Ξ_{AB} for pre-flowed configurations is closer to 1 than it without pre-flowed. Left: conf.1. Right: conf.2.

V. TOPOLOGICAL CHARGE DENSITY CORRELATOR AND THE PSEUDOSCALAR GLUEBALL MASS

The TCDC is given by [12]

$$C(r) = \langle q(x) q(0) \rangle, \quad r = |x|, \quad (21)$$

where $q(x)$ is the topological charge density. Due to the reflection positivity and the pseudoscalar nature of the relevant local operator in Euclidean field theory, TCDC is negative at nonzero distances. TCDC can be used to extract the lowest pseudoscalar glueball mass in the negative region by the following form [41]:

$$\langle q(x) q(0) \rangle = \frac{m}{4\pi^2 r} K_1(mr), \quad (22)$$

and $K_1(z)$ is a modified Bessel function, which has the asymptotic form

$$K_1(z) \underset{\text{large } z}{\sim} e^{-z} \sqrt{\frac{\pi}{2z}} \left[1 + \frac{3}{8z} \right]. \quad (23)$$

Owing to the TCDC has severe singularities and lattice artifacts, a smoothing procedure is needed to smooth the gauge fields. In this work, we will use Wilson flow to smooth the gauge field. Undersmearing can not remove the lattice artifacts enough, while oversmearing may eliminate even the negativity character of the TCDC, shown in Fig. 12. It shows that the negative dip disappears when the flow radius is about $\sqrt{8\tau} = 0.21$ fm. Therefore, it is very important that how much Wilson flow time τ to take at which the configurations

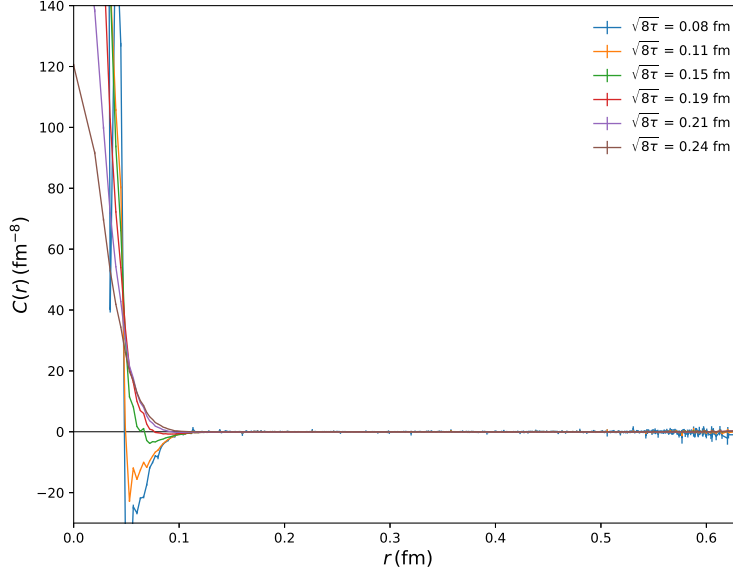


Figure 12: $C(r)$ versus r at various value of the Wilson flow time $\sqrt{8\tau}$. When the Wilson flow time is small, $C(r)$ are very noise. However, too large Wilson flow time eliminate the negativity of TCDC. The negative dip wipe out when the flow radius is about 0.21 fm.

are smoothed properly. In order to get the proper Wilson flow time, Ref. [19] proposed to use the stability of the topological susceptibility to figure out the lower bound for the Wilson flow time at finite temperature. In this work, we will compare this method with the matching procedure discussed in the previous section to get the proper Wilson flow time τ for the calculation of topological charge density. In the calculation of TCDC, we choose $\epsilon = 0.02$, the total flow time $\tau = 1.0$ and a proper τ to calculated $q(x)$, and the number of configurations is 500.

The topological susceptibility χ in Euclidean space-time is defined by

$$\chi = \int d^4x \langle q(x) q(0) \rangle = \frac{\langle Q^2 \rangle}{V}, \quad V \rightarrow \infty, \quad (24)$$

where Q is the topological charge,

$$Q = \int d^4x q(x). \quad (25)$$

In Fig. 13, the topological susceptibility χ is shown with respect to the Wilson flow time τ . We observe that as the flow time τ increased, the UV-fluctuations are more smoothed

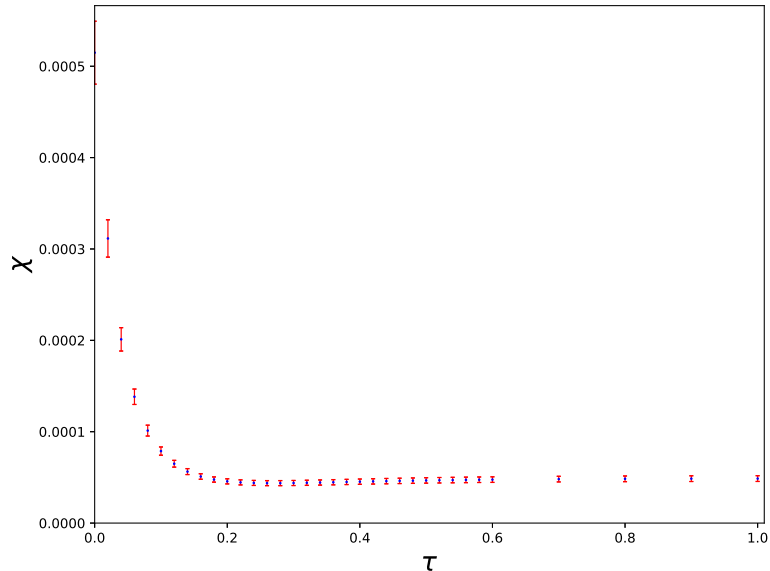


Figure 13: χ for different flow time τ in lattice unit. With enough large τ , χ remains almost constant. The number of configurations is 500.

out and the susceptibility reaches a plateau. We find that $\tau \approx 0.2$ seems to be the lower bound of the flow time for this zero temperature case, which is smaller than the proper flow time $\tau = 0.32$ obtained by the matching procedures in the previous analysis. In this work, we used $\tau = 0.32$ as the best flow time for calculating the TCDC from bosonic definition.

Next we will try to extract the glueball mass from the TCDC with Wilson flow time $\tau \approx 0.32$. We use Eq. (22) and (23) to extract the pseudoscalar glueball mass in the large- r region. In this fitting procedure, the amplitude and mass are treated as free parameters. TCDC and the fitting curve with $\tau = 0.32$ as an example are shown in Fig. 14.

We find that while the error bar of the tail of TCDC touches the value zero, the extracted mass is independent of the ending point. Then we fix the ending point and vary the starting point to extract the mass, shown in Fig. 15. We find that the most stable fitting plateau is $r/a \in [4.0, 5.29]$ shown by the range of the magenta dashed line in Fig. 15 [42]. Then we do the fitting in the most stable fitting window. The numerical value of the pseudoscalar glueball mass is $M = 2558(114)$ MeV represented by the cyan solid line and the magenta lines represent the errors of the final pseudoscalar glueball mass in Fig. 15, which is consistent with the results in Ref. [14, 43].

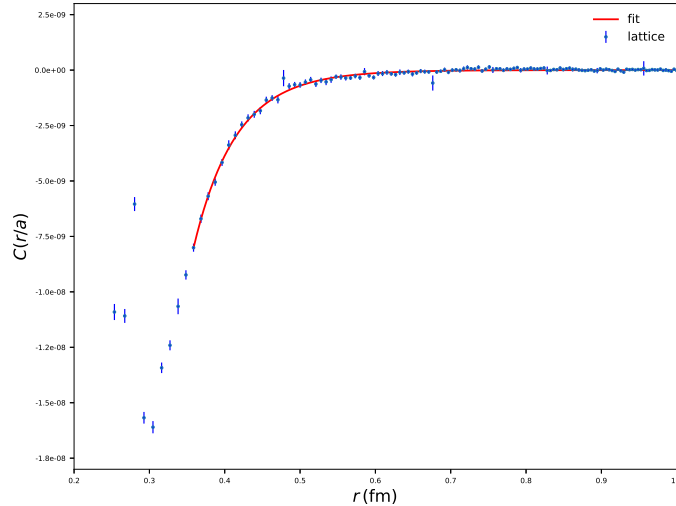


Figure 14: $C(r/a)$ versus r at Wilson flow time $\tau = 0.32$. The fitting curve to extract the pseudoscalar glueball mass is also shown.

VI. CONCLUSIONS

We have analysed the topological charge density $q(x)$ using direct visualizations. We find that the SMP method is a good choice to study the topological charge density. The results show that the topological charge density depends on the Wilson mass parameter m in the fermionic definition. By comparing the $q_{\text{smp}}(x)$ with the gluonic definition of $q_{\text{wf}}(x)$, a correlation between m and n_{wf} is revealed. Smaller values of κ remove non-trivial topological charge fluctuations, which are similar to smoothing the configuration with a large Wilson flow time. By analysing the topological charge density $q(x)$, we find that the best matching number of Wilson flow for the gluonic definition of topological charge density can be obtained by the comparison of $q_{\text{smp}}(x)$ with $q_{\text{wf}}(x)$.

We used the SMP method to a pre-flowed gauge field. It shows that the pre-flowed process will remove the non-trivial topological density fluctuations. We also find that UV-filtering still occurs in the SMP topological charge density and more Wilson flow time is required to match the $q_{\text{smp}}(x)$. Q for pre-flowed configurations more likely tend to the same integer value than the original configurations when κ varies.

We have studied the TCDC and analysed the topological susceptibility χ . It indicates

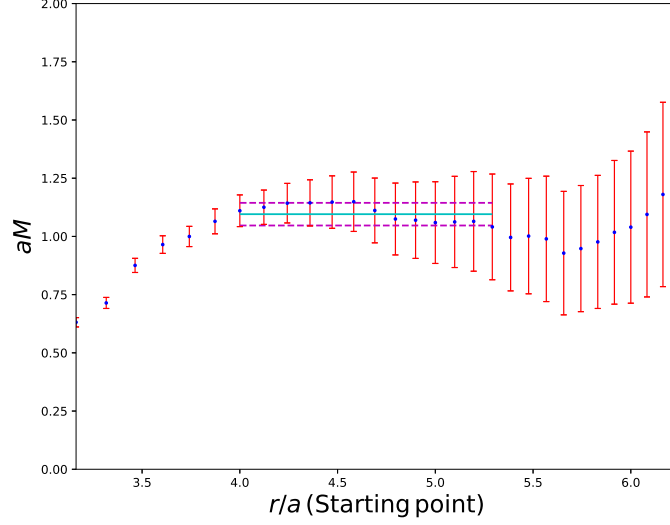


Figure 15: The pseudoscalar glueball mass with varied starting point. The range of magenta dashed lines show the most stable fitting plateau.

that the topological susceptibility χ indeed reaches to a plateau for the large enough Wilson flow time. At the same time, the best matching number of Wilson flow for the calculation of the topological charge density based on bosonic definition can be obtained. However, it finds that the best flow time by the matching procedures is larger than the lower bound of the flow time by analyzing the topological susceptibility for the zero temperature case. We also extract the pseudoscalar glueball mass at the best Wilson flow time determined by matching procedures. In the future work, we should perform more configurations, larger lattice or a continuum extrapolation.

Acknowledgments

Numerical simulations have been performed on the Tianhe-2 supercomputer at the National Supercomputer Center in Guangzhou(NSCC-GZ), China. This work is supported by

the National Natural Science Foundation of China (NSFC) under the project No. 11335001.

- [1] G. Schierholz, *Towards a dynamical solution of the strong CP problem*, *Nucl. Phys. Proc. Suppl.* **37A** (1994) 203–210 [[hep-lat/9403012](#)].
- [2] Edward Witten, *Instantons, the Quark Model, and the $1/N$ Expansion*, *Nucl. Phys. B* **149** (1979) 285–320.
- [3] Dmitri Diakonov, *Chiral symmetry breaking by instantons*, *Proc. Int. Sch. Phys. Fermi* **130** (1996) 397–432 [[hep-ph/9602375](#)].
- [4] Krzysztof Cichy, Arthur Dromard, Elena Garcia-Ramos, Konstantin Ottnad, Carsten Urbach, Marc Wagner, Urs Wenger, and Falk Zimmermann, *Comparison of different lattice definitions of the topological charge*, *PoS LATTICE2014* (2014) 075 [[1411.1205](#)].
- [5] M. Müller-Preussker, *Recent results on topology on the lattice (in memory of Pierre van Baal)*, *PoS LATTICE2014* (2015) 003 [[1503.01254](#)].
- [6] Constantia Alexandrou, Andreas Athenodorou, Krzysztof Cichy, Arthur Dromard, Elena Garcia-Ramos, Karl Jansen, Urs Wenger, and Falk Zimmermann, *Comparison of topological charge definitions in Lattice QCD*, *Eur. Phys. J. C* **80** (2020) 424 [[1708.00696](#)].
- [7] M. F. Atiyah and I. M. Singer, *The Index of elliptic operators. 5.*, *Annals Math.* **93** (1971) 139–149.
- [8] Peter Hasenfratz, Victor Laliena, and Ferenc Niedermayer, *The Index theorem in QCD with a finite cutoff*, *Phys. Lett. B* **427** (1998) 125–131 [[hep-lat/9801021](#)].
- [9] A.A. Belavin, Alexander M. Polyakov, A.S. Schwartz, and Yu.S. Tyupkin, *Pseudoparticle Solutions of the Yang-Mills Equations*, *Phys. Lett. B* **59** (1975) 85–87.
- [10] Kazuo Fujikawa, *A continuum limit of the chiral jacobian in lattice gauge theory*, *Nucl. Phys. B* **546** (1999) 480–494.
- [11] Yoshio Kikukawa and Atsushi Yamada, *Weak coupling expansion of massless QCD with a Ginsparg-Wilson fermion and axial $U(1)$ anomaly*, *Phys. Lett. B* **448** (1999) 265–274 [[hep-lat/9806013](#)].
- [12] Abhishek Chowdhury, Asit K. De, A. Harindranath, Jyotirmoy Maiti, and Santanu Mondal, *Topological charge density correlator in Lattice QCD with two flavours of unimproved Wilson fermions*, *JHEP* **11** (2012) 029 [[1208.4235](#)].

- [13] Michael Creutz, *Anomalies, gauge field topology, and the lattice*, *Annals Phys.* **326** (2011) 911–925 [1007.5502].
- [14] Abhishek Chowdhury, A. Harindranath, and Jyotirmoy Maiti, *Correlation and localization properties of topological charge density and the pseudoscalar glueball mass in $su(3)$ lattice yang-mills theory*, *Phys. Rev. D* **91** (2015) 074507 [1409.6459].
- [15] Jan Smit and Jeroen C. Vink, *Remnants of the Index Theorem on the Lattice*, *Nucl. Phys. B* **286** (1987) 485–508.
- [16] Martin Lüscher and Filippo Palombi, *Universality of the topological susceptibility in the $SU(3)$ gauge theory*, *JHEP* **09** (2010) 110 [1008.0732].
- [17] Edward Witten, *Current Algebra Theorems for the $U(1)$ Goldstone Boson*, *Nucl. Phys. B* **156** (1979) 269–283.
- [18] G. Veneziano, *$U(1)$ Without Instantons*, *Nucl. Phys. B* **159** (1979) 213–224.
- [19] Lukas Mazur, Luis Altenkort, Olaf Kaczmarek, and Hai-Tao Shu, *Euclidean correlation functions of the topological charge density*, *PoS LATTICE2019* (2020) 219 [2001.11967].
- [20] Herbert Neuberger, *Exactly massless quarks on the lattice*, *Phys. Lett. B* **417** (1998) 141–144 [hep-lat/9707022].
- [21] Herbert Neuberger, *More about exactly massless quarks on the lattice*, *Phys. Lett. B* **427** (1998) 353–355 [hep-lat/9801031].
- [22] I. Horváth, S.J. Dong, Terrence Draper, F.X. Lee, K.F. Liu, N. Mathur, H.B. Thacker, and J.B. Zhang, *Low dimensional long range topological charge structure in the QCD vacuum*, *Phys. Rev. D* **68** (2003) 114505 [hep-lat/0302009].
- [23] E.-M. Ilgenfritz, K. Koller, Y. Koma, G. Schierholz, T. Streuer, and V. Weinberg, *Exploring the structure of the quenched QCD vacuum with overlap fermions*, *Phys. Rev. D* **76** (2007) 034506 [0705.0018].
- [24] Guang-Yi Xiong, Jian-Bo Zhang, and You-Hao Zou, *Evaluating the topological charge density with the symmetric multi-probing method*, *Chin. Phys. C* **43(3)** (2019) 033102.
- [25] Rajamani Narayanan and Herbert Neuberger, *A Construction of lattice chiral gauge theories*, *Nucl. Phys. B* **443** (1995) 305–385 [hep-th/9411108].
- [26] Robert G. Edwards, Urs M. Heller, and Rajamani Narayanan, *Spectral flow, chiral condensate and topology in lattice QCD*, *Nucl. Phys. B* **535** (1998) 403–422 [hep-lat/9802016].
- [27] Rajamani Narayanan and Pavlos M. Vranas, *A Numerical test of the continuum index*

- theorem on the lattice*, *Nucl. Phys. B* **506** (1997) 373–386 [[hep-lat/9702005](#)].
- [28] J.B. Zhang, S.O. Bilson-Thompson, F.D.R. Bonnet, D.B. Leinweber, Anthony G. Williams, and J.M. Zanotti, *Numerical study of lattice index theorem using improved cooling and overlap fermions*, *Phys. Rev. D* **65** (2002) 074510 [[hep-lat/0111060](#)].
 - [29] Hans Mathias Mamen Vege, *Solving $SU(3)$ Yang-Mills theory on the lattice: a calculation of selected gauge observables with gradient flow*, *Master’s thesis* (2019) U. Oslo (main).
 - [30] Peter J. Moran, Derek B. Leinweber, and Jianbo Zhang, *Wilson mass dependence of the overlap topological charge density*, *Phys. Lett. B* **695** (2011) 337–342 [[1007.0854](#)].
 - [31] M. Lüscher and P. Weisz, *On-Shell Improved Lattice Gauge Theories*, *Commun. Math. Phys.* **97** (1985) 59 [Erratum: *Commun. Math. Phys.* **98** (1985) 433].
 - [32] Frederic D.R. Bonnet, Derek B. Leinweber, Anthony G. Williams, and James M. Zanotti, *Improved smoothing algorithms for lattice gauge theory*, *Phys. Rev. D* **65** (2002) 114510 [[hep-lat/0106023](#)].
 - [33] Zhen Cheng, Jian-Bo Zhang, and Guang-Yi Xiong, *Calculation of disconnected quark loops in lattice QCD*, *Chin. Phys. C* **44(3)** (2020) 033104.
 - [34] Pilar Hernandez, Karl Jansen, and Martin Luscher, *Locality properties of Neuberger’s lattice Dirac operator*, *Nucl. Phys. B* **552** (1999) 363–378 [[hep-lat/9808010](#)].
 - [35] Martin Lüscher, *Properties and uses of the Wilson flow in lattice QCD*, *JHEP* **08** (2010) 071 [Erratum: *JHEP* **03** (2014) 092]. [[1006.4518](#)].
 - [36] Claudio Bonati and Massimo D’Elia, *Comparison of the gradient flow with cooling in $SU(3)$ pure gauge theory*, *Phys. Rev. D* **89** (2014) 105005 [[1401.2441](#)].
 - [37] Sundance O. Bilson-Thompson, Derek B. Leinweber, and Anthony G. Williams, *Highly improved lattice field strength tensor*, *Annals Phys.* **304** (2003) 1–21 [[hep-lat/0203008](#)].
 - [38] Falk Bruckmann, Christof Gattringer, Ernst-Michael Ilgenfritz, Michael Muller-Preussker, Andreas Schafer, and Stefan Solbrig, *Quantitative comparison of filtering methods in lattice QCD*, *Eur. Phys. J. A* **33** (2007) 333–338 [[hep-lat/0612024](#)].
 - [39] Sundance O. Bilson-Thompson, Derek B. Leinweber, Anthony G. Williams, and Gerald V. Dunne, *Comparison of $|Q| = 1$ and $|Q| = 2$ gauge-field configurations on the lattice four-torus*, *Annals Phys.* **311** (2004) 267–287 [[hep-lat/0306010](#)].
 - [40] Colin Morningstar and Mike J. Peardon, *Analytic smearing of $SU(3)$ link variables in lattice QCD*, *Phys. Rev. D* **69** (2004) 054501 [[hep-lat/0311018](#)].

- [41] Edward V. Shuryak and J.J.M. Verbaarschot, *Screening of the topological charge in a correlated instanton vacuum*, *Phys. Rev. D* **52** (1995) 295–306 [[hep-lat/9409020](#)].
- [42] You-Hao Zou, Jian-Bo Zhang, and Guang-Yi Xiong, *Localization of topological charge density near T_c in quenched QCD with Wilson flow*, *Phys. Rev. D* **98** (2018) 014504 [[1806.05301](#)].
- [43] Y. Chen et al, *Glueball spectrum and matrix elements on anisotropic lattices*, *Phys. Rev. D* **73** (2006) 014516 [[hep-lat/0510074](#)].